Phosphino-indenyl complexes of nickel(II)[1]

Laurent F. Groux, Francine Bélanger-Gariépy, and Davit Zargarian

Abstract: The BH_3-protected phosphinoindenyl ligand indenyl$(CH_2)_2PPh_2{\cdot}BH_3$ was used in the preparation of ($\eta^{5/3}$:η^0-indenyl$(CH_2)_2PPh_2{\cdot}BH_3$)Ni(PPh_3)Cl, which has been characterized by NMR spectroscopy and X-ray diffraction studies. On the other hand, all attempts at preparing the closely related complex ($\eta^{5/3}$:η^1-indenyl$(CH_2)_2PPh_2$)NiCl, in which the tethered phosphine moiety is coordinated to the Ni centre, were unsuccessful. One of these unsuccessful attempts yielded instead the novel indenyl-PCP pincer complex {κ^P,κ^C,κ^P-1,3-$(CH_2CH_2PPh_2)_2$-2-indenyl}NiCl, which has been characterized by X-ray diffraction studies.

Key words: indenyl complexes, tethered phosphines, PCP pincer complexes.

Résumé : Le ligand protégé indenyl$(CH_2)_2PPh_2{\cdot}BH_3$ a permis la préparation du composé ($\eta^{5/3}$:η^0-indenyl$(CH_2)_2$-$PPh_2{\cdot}BH_3$)Ni(PPh_3)Cl. Ce dernier a été complètement caractérisé par la spectroscopie RMN et études cristallographiques. Toutes les tentatives de préparer et isoler le complexe ($\eta^{5/3}$:η^1-indenyl$(CH_2)_2PPh_2$)NiCl ont échoué. En revanche, nous avons obtenu lors d'une de ces tentatives un nouveau complexe inattendu; une étude cristallographique a démontré que ce dernier était un complexe de type « pincer » PCP-indényle, soit {κ^P,κ^C,κ^P-1,3-$(CH_2CH_2PPh_2)_2$-2-indenyl}NiCl.

Mots clés : complexes d'indényle, phosphines attachées, complexe de type « pincer » PCP.

Introduction

Previous studies have shown that the complexes (Ind)Ni(PR_3)X (Ind = indenyl and its substituted derivatives; R = Ph, Me, Cy; X = Cl, Me, CC-Ph, etc.) (1) are active precatalysts for the oligo- and polymerization of alkenes (2), alkynes (3), and $PhSiH_3$ (4) and the hydrosilylation of olefins and ketones (5). The available mechanistic evidence indicates that the steric and (or) electronic properties of the phosphine ligand and its relative lability influence the rates of these reactions and the catalytic activities. Thus, the PMe_3 derivatives are much more active than their PPh_3 analogues in the polymerization of ethylene (2*a*) and $PhSiH_3$ (4), whereas the opposite order of reactivity is found in the hydrosilylation reactions (5).

To examine further the influence of phosphines on the above reactions, we considered studying a series of complexes featuring ligands of the type Ind^PR_2, with ^ representing a side chain connecting the PR_2 and Ind moieties. Our reasoning was that since the chelating phosphine moiety in (Ind^PR_2)NiX should be less prone to dissociation, studying the reactivities of such complexes should allow a direct measure of the impact of phosphine lability on the reactivities of this family of complexes. A search of the literature showed that complexes bearing the analogous Cp^PR_2 ligands are known for many transition metals (except those of group 10) (6), whereas complexes of Ind^PR_2 ligands are known only for Cr (7), Ru (8), Rh (9), and Ir (9*b*). Therefore, we set out to prepare (Ind^PR_2)NiX and probe the influence of the chelating PR_2 moiety on reactivities. The present report describes our attempts to prepare the complex ($\eta^{5/3}$:η^1-Ind$CH_2CH_2PPh_2$)NiCl.

Results and discussion

The ligand Ind$(CH_2)_2PPh_2$ (**1**) was prepared by slightly modified versions of previously reported procedures (10, 11), consisting of (*a*) successive nucleophilic displacements of Cl^- in $ClCH_2CH_2Cl$ by $[PPh_2]^-$ and $[Ind]^-$ or (*b*) the reductive cleavage of spiro(cyclopropane-1,1′-indene) (12) by $[PPh_2]^-$ (Scheme 1). Crude samples of **1** obtained from these routes were reacted with $BH_3{\cdot}THF$ to protect the phosphine moiety from oxidation; pure samples of Ind$(CH_2)_2PPh_2{\cdot}BH_3$ (**1**·BH_3) were then isolated by flash chromatography and completely characterized by NMR and X-ray diffraction studies (13). Treatment of **1**·BH_3 with H^+, followed by neutralization with Na_2CO_3, removed the protecting group and gave pure samples of **1**, which were used in subsequent experiments. Alternatively, crude samples of **1** were used in a few instances for the preparation of the target complex; for this purpose, route (*b*) proved more convenient because the in situ generated anion $[Ind(CH_2)_2PPh_2]^-$ obviated the need for an additional deprotonation step.

Received 1 December 2004. Published on the NRC Research Press Web site at http://canjchem.nrc.ca on 9 June 2005.

This contribution is dedicated to Professor H. Alper in recognition of his seminal contributions to organometallic catalysis.

L.F. Groux, F. Bélanger-Gariépy, and D. Zargarian.[2] Département de chimie, Université de Montréal, Montréal, QC H3C 3J7, Canada.

[1]This article is part of a Special Issue dedicated to Professor Howard Alper.
[2]Corresponding author (e-mail: zargarian.davit@umontreal.ca).

 doi: 10.1139/V05-079

Scheme 1.

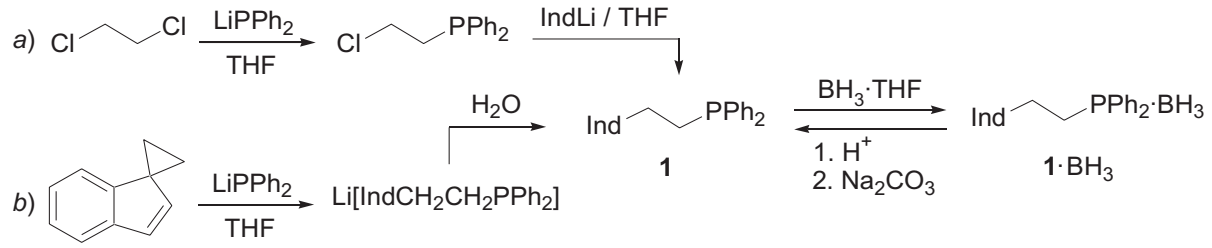

Scheme 2.

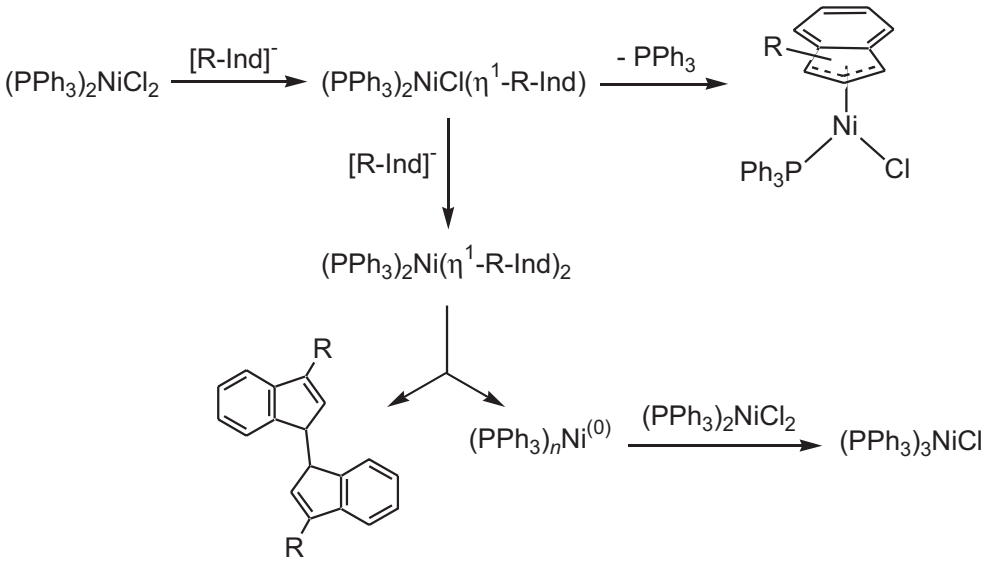

The main synthetic route used for the attempted synthesis of the target complex was based on the procedure used for the preparation of IndNi(PR_3)Cl (14). Thus, ligand **1** was deprotonated with BuLi and added to an Et_2O suspension of Ni(PPh_3)$_2Cl_2$. This addition changed the forest-green colour of the initial mixture to dark red, the typical colour of IndNi(PR_3)Cl; shortly thereafter, however, the reaction mixture turned beige-brown and a beige solid precipitated, implying the onset of a decomposition process. The $^{31}P\{^1H\}$ NMR spectrum of the filtrate obtained from filtration of the final mixture showed that the reaction had produced a number of phosphine-containing species,[3] while the observation of several broad signals in the ^1H NMR spectrum indicated that one or more paramagnetic species had also formed. The ^1H NMR spectrum of the beige solid obtained from the filtration also showed broad and featureless signals. Cooling the beige filtrate yielded yellow crystals that were identified as the Ni(I) complex (PPh_3)$_3$NiCl (15). The formation of this species has been observed in previous studies (16) and signals a side reaction involving the nickel-catalyzed coupling of two indenyl ligands (Scheme 2).

The above procedure was repeated several times under different reaction conditions (e.g., solvent, temperature, order of mixing, source of nickel, etc.), but no set of conditions allowed the successful isolation of ($\eta^{5/3}$:η^1-IndCH_2CH_2-PPh_2)NiCl. The precise reasons for the failure to obtain our target complex are not known; we speculate, however, that the dark-red species formed during the initial stages of these reactions is an intermediate species such as ($\eta^{5/3}$:η^0-Ind-$CH_2CH_2PPh_2$)Ni(PPh_3)Cl, **2**. The apparent instability of this species is in contrast to the stability of the analogous complexes ($\eta^{5/3}$:η^0-Ind^NR_2)Ni(PPh_3)Cl, which have been synthesized successfully (2*c*, 17). The discrepancy in the stabilities of these complexes leads us to suspect that the pitfall of our synthetic approach lies with the incompatible intramolecular interaction of the chelating phosphine moiety with the Ni centre.

The above hypothesis was borne out by the finding that the above-proposed intermediate is indefinitely stable when the PPh_2 moiety is coordinated by BH_3. Thus, using the BH_3-protected ligand **1**·BH_3 in our syntheses allowed the successful isolation of the complex ($\eta^{3/5}$:η^0-IndCH_2CH_2-PPh_2·BH_3)Ni(PPh_3)Cl, **2**·BH_3 (Scheme 3). The structure proposed for this complex was corroborated by the NMR spectra, as follows. For instance, the $^{31}P\{^1H\}$ NMR spectrum of **2**·BH_3 showed a sharp singlet at 29.9 ppm (parts per million), attributed to the Ni-PPh_3 moiety; for comparison, the corresponding signal in (Ind-$CH_2CH_2NMe_2$)Ni(PPh_3)Cl

[3] The $^{31}P\{^1H\}$ NMR spectrum (C_6D_6) displayed the following signals: 44.6, 33.6, 33.3, 32.8, 32.5, 30.3, 30.1, 29.9, 29.4, 29.1, 24.4 (O=PPh_3), 20.7, 3.2, –4.9 (free PPh_3). The signals displayed in the corresponding spectrum in $CDCl_3$ were as follows: 58.7, 57.9, 55.9, 34.2, 33.6, 32.5, 30.2, 29.5 (O=PPh_3), 24.8, 23.3, 21.6, 20.2, –3.5, –4.8 (free PPh_3), –14.0, –15.0.

Scheme 3.

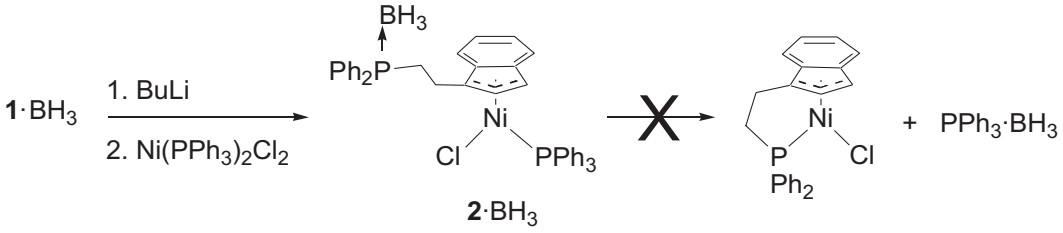

Scheme 4.

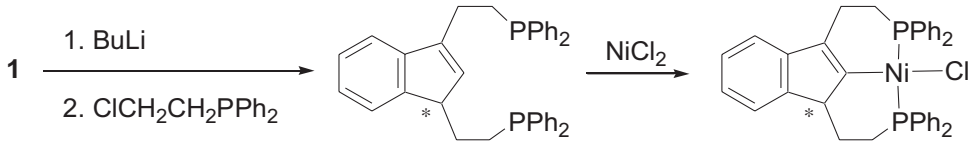

Fig. 1. ORTEP plot of **2**·BH_3. Hydrogen atoms have been omitted for clarity. Selected distances (Å) and angles (°): Ni—Cl 2.143(7), Ni—C2 2.054(6), Ni—C3 2.031(7), Ni—C3A 2.321(7), Ni—C7A 2.365(8), Ni—P1 2.179(3), Ni—Cl 2.170(2), C1—C2 1.435(8), C2—C3 1.419(8), C3—C3A 1.397(9), C3A—C7A 1.439(9), C7A—C1 1.462(8), P2—B 1.912(8); C1-Ni-P1 164.0(2), C3-Ni-C1 160.0(2), P1-Ni-C1 101.09(9), C1-Ni-C1 94.7(2), P1-Ni-C3 98.0(2), C1-Ni-C3 66.0(3).

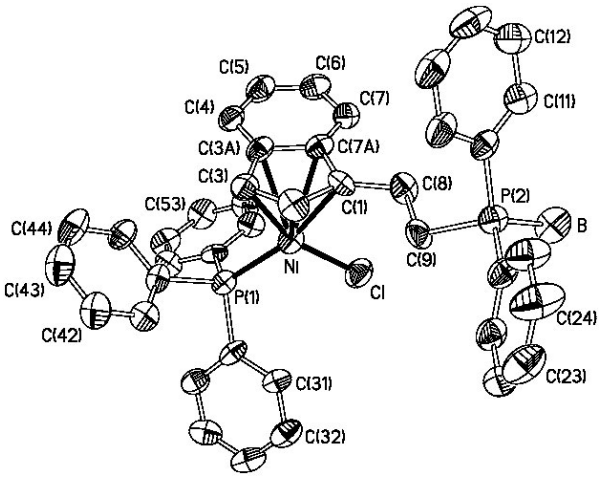

resonates at 30.8 ppm (see ref. 17*a*). In addition, we observed a peak at 17.5 ppm that was broadened as a result of coupling to the quadrupolar ^{11}B nucleus (cf. **1**·BH_3: 16.6 ppm). The ^1H NMR spectrum contained a broad singlet at ca. 1.2 ppm assigned to BH_3, in addition to the characteristic signals for the Ind protons (e.g., a signal at ca. 3.5 ppm assigned to H3). The unequivocal confirmation of the proposed structure was furnished by the results of X-ray diffraction studies, described below.

Complex **2**·BH_3 adopts virtually the same structure as many of the previously reported Ni-indenyl complexes (1). The coordination geometry around Ni (Fig. 1) can be described as a distorted square-planar geometry with the indenyl ligand perpendicular to the coordination plane. The tethered Ph_2P·BH_3 moiety points away from the metal centre, and the absence of any P–Ni interaction results in a virtually unchanged P—BH_3 distance (1.912(3) Å in **2**·BH_3 vs. 1.923(3) Å in **1**·BH_3). The Ind hapticity is distorted toward an unsymmetrical, trihapto mode, as reflected in the following structural parameters: (*i*) the Ni—C3a and Ni—C7a bond distances (avg. 2.34 Å) are much longer than the Ni—C1 and Ni—C3 distances (avg. 2.08 Å); (*ii*) the Ni—C1 distance (ca. 2.14 Å) is significantly longer than the Ni—C3 distance (ca. 2.03 Å); (*iii*) the slip parameters[4] Δ(M—C) (0.26 Å), HA (ca. 8.7°), and FA (ca. 8.3°) are in the expected range for η^5/η^3-Ind ligands (18). This type of "slippage" is attributed to (*a*) the tendency of Ni(II) to avoid an 18-electron configuration and (*b*) the different trans influences of PPh_3 and Cl ligands, respectively (1).

With complex **2**·BH_3 at hand, we attempted to prepare **2** by thermally inducing the transfer of BH_3 from the tethered PPh_2 moiety to the PPh_3 ligand and the subsequent elimination of Ph_3P·BH_3; unfortunately, however, no BH_3-exchange was observed between the phosphine moieties. On the other hand, direct deprotection of the tethered PPh_2 moiety by amines led instead to decomposition. It appears, therefore, that the target complex ($\eta^{5/3}$:η^1-Ind$CH_2CH_2PPh_2$)NiCl is inherently unstable. Although modeling studies do not support the hypothesis that this instability is caused by the CH_2CH_2 tether, future attempts will investigate the feasibility of preparing analogous complexes bearing longer side chains.

A new PCP–Ni complex

One of the attempts to synthesize the target complex resulted in the unexpected formation of a Ni complex bearing the new ligand Ph_2P^Ind^PPh_2, shown in Scheme 4. Thus, reacting $NiCl_2$ with a crude batch of **1**, prepared according to route (*a*) in Scheme 1, gave a red mixture that yielded a small quantity of red crystals identified by X-ray diffraction studies as the novel pincer complex (PCP-Ind($(CH_2)_2$-$PPh_2)_2$)NiCl, **3**. The $^{31}P\{^1H\}$ NMR spectrum of **3** showed two AB doublets displaying large coupling constants ($^2J_{P\text{-}P}$ =

[4] These slip parameters are defined as follows: ΔM—C = 1/2[(M—C3a + M—C7a) – (M—C1 + M—C3)]; HA is the angle between the planes formed by the atoms C(1), C(2), C(3) and C(1), C(3), C(3a), C(7a); FA is the angle between the planes formed by the atoms C(1), C(2), C(3) and C(3a), C(4), C(5), C(6), C(7), and C(7a).

Fig. 2. ORTEP plot of **3**. Hydrogen atoms and disordered solvent have been omitted for clarity. Selected distances (Å) and angles (°): Ni—Cl 2.2086(12), Ni—P1 2.1772(10), Ni—P2 2.2146(9), Ni—C2 1.888(3), C1—C2 1.525(4), C2—C3 1.360(4), C3—C3A 1.457(4), C3A—C7A 1.391(5), C1—C7A 1.522(4); C1-Ni-P1 98.32(4), C1-Ni-P2 91.95(4), C2-Ni-P1 85.08(9), C2-Ni-P2 88.96(9), C1-Ni-C2 162.46(9), P1-Ni-P2 163.64(3).

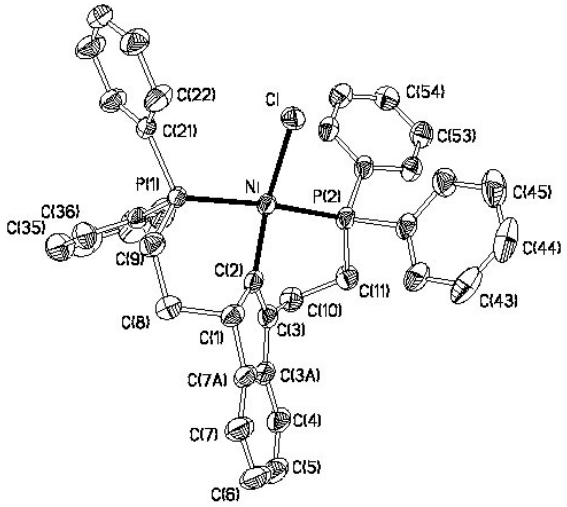

330 Hz), indicative of inequivalent trans phosphine moieties. The ^{1}H NMR spectrum displayed a broad singlet at ca. 3.6 ppm, which was assigned to H1, in addition to a number of multiplets in the aromatic and aliphatic regions; the latter are assigned to the chemically inequivalent[5] protons on the ethyl side chains.

X-ray diffraction studies showed that the coordination geometry around the Ni centre in **3** is slightly distorted square planar (Fig. 2), the main source of distortion arising from inter-ligand angles of ca. 163° for the trans ligands and 98°–85° for the cis ligands. Two trans coordination sites are occupied by the PPh_2 moieties, which form unequal Ni—P bond lengths (ca. 2.177 and 2.215 Å). The presence of an asymmetric centre at C1 results in the formation of two enantiomers, but the molecule crystallizes in the centrosymmetric space group $P\bar{1}$ because these enantiomers exist in a racemic mixture.

The most novel feature of complex **3** is the 2-indenyl ligand that is η^1-bonded to Ni via C2 (Ni—C(sp^2) = 1.89 Å). The localized nature of bonding within the 5-membered ring portion of the Ind ligand is evident from the much longer bond lengths for C1—C2 (1.525(4) Å), C7a—C1 (1.522(4) Å), and C3—C3a (1.457(4) Å) compared with C2—C3 (1.360(4) Å). We believe that **3** is the first isolated η^1-indenyl nickel complex and one of very few 2-η^1-indenyl complexes ever reported (19). The unanticipated formation of this compound likely results from the side reactions shown in Scheme 4: a small amount of deprotonated **1** reacts with a second equivalent of $ClCH_2CH_2PPh_2$ to give the doubly functionalized indene, 1,3-$(CH_2CH_2PPh_2)_2$IndH; the latter then reacts with $NiCl_2$ by C-H activation at the 2-position to give **3**.

Pincer compounds have attracted much attention recently owing to the many interesting reactions they promote and (or) catalyze (20), including alkane dehydrogenations (21), ketone hydrogenations (22), Heck coupling (23), olefin aminations (24), etc. (25). Most pincer complexes have a C_2 symmetric skeleton based on an *ortho*,*ortho*-disubstituted aryl ring, a 1,5-disubstituted pentyl chain, or a 1,3-disubstituted Cp moiety; what sets complex **3** apart is the presence of an optically active centre at C1. Efforts are underway to develop a reliable and high-yielding synthetic route for ligands of the type R_2P^Ind^PR_2 and their complexes. The reactivities of these complexes will then be investigated with a view to exploiting the optically active character of this type of PCP complex.

Concluding remarks

The results described in this paper indicate that ($\eta^{3/5}$:η^0-$IndCH_2CH_2PPh_2$·BH_3)$Ni(PPh_3)Cl$ owes its stability to the protection of the PPh_2 moiety by BH_3, because all attempts at preparing the original target complex wherein PPh_2 is coordinated to the Ni centre led to decomposition. We conclude, therefore, that tethering the phosphine moiety to the Ind ligand has a destabilizing effect on the complexes $IndNi(PR_3)Cl$. In contrast, many related complexes are stable and isolable (e.g., (η^5:η^1-Ind^PPh_2)$Rh^I(CO)$ (9), (η^5:η^1-Ind^PPh_2)Rh^{III}(C(=O)R)X (R = Me, Et; X = Br, I) (26), and (η^5:η^1-Ind^PR_2)Cr(X)Cl (X = Cl, Me) (7)), implying that the chelation of the tethered phosphine is not inherently destabilizing in all cases. It remains to be seen whether Ni complexes of Ind^PR_2 bearing longer tethers will be stable to isolation.

Experimental

General considerations

All manipulations were performed under an inert atmosphere of N_2 using standard Schlenk techniques and a drybox. Dry, oxygen-free solvents were employed throughout. Ind$(CH_2)_2PPh_3$ (**1**) has been prepared according to modified procedures (11, 12). All other reagents used in the experiments were obtained from commercial sources and used as received. The NMR spectra were recorded on a Bruker AMXR400 spectrometer (^{1}H (400 MHz), ^{13}C{^{1}H} (100.56 MHz), and ^{31}P{^{1}H} (161.92 MHz)).

Preparation of 2·BH_3

BuLi (0.47 mL of a 2.5 mol/L solution in hexane) was added to a solution of **1**·BH_3 (400 mg, 1.17 mmol) in Et_2O (200 mL) and stirred for 2 h. This solution was then added dropwise to a suspension of $Ni(PPh_3)_2Cl_2$ (1.48 g, 2.27 mmol) in Et_2O (50 mL), whereupon the solution turned dark red immediately. The mixture was evaporated, and the residues were dissolved in CH_2Cl_2 (30 mL); diluting this solution with hexane (120 mL) and storing the mixture at –20 °C gave a dark red solid precipitate (450 mg, 55% yield). ^{1}H NMR ($CDCl_3$): 7.9–7.2 (PPh_3 and PPh_2), 7.16 (t, $^3J_{H\text{-}H}$ = 7.4 Hz, H6), 7.09 (d, $^3J_{H\text{-}H}$ = 8.0 Hz, H7), 6.91 (t, $^3J_{H\text{-}H}$ = 7.3 Hz, H5), 6.56 (d, $^3J_{H\text{-}H}$ = 3.0 Hz, H2), 6.08 (d,

[5] The rigid geometry imposed by the chelating PPh_2 moieties and the presence of an asymmetric centre at C1 render the methylene protons diastereotopic.

Table 1. Crystal data, data collection, and structure refinement of **2** and **3**.

	2	**3**
Formula	$C_{41}H_{38}BP_2ClNi$	$C_{37}H_{33}P_2ClNi{\cdot}CH_2Cl_2$
Color and habit	Dark red block	Red plate
Dimensions (mm^3)	0.31×0.19×0.04	0.37×0.31×0.14
Symmetry	Triclinic	Triclinic
Space group	$P\bar{1}$	$P\bar{1}$
a (Å)	8.952(5)	10.741(4)
b (Å)	13.245(9)	12.875(3)
c (Å)	15.670(8)	14.361(6)
α (°)	84.66(4)	65.63(3)
β (°)	74.67(4)	73.92(3)
γ (°)	81.02(5)	77.76(2)
Volume ($Å^3$)	1767.3(18)	1727.4(10)
Z	2	2
D_{calcd} (g cm^{-1})	1.311 0	1.382
Diffractometer	Nonius CAD-4	Nonius CAD-4
Temp (K)	293(2)	293(2)
λ (Cu Kα) (Å)	1.541 78	1.540 56
μ (mm^{-1})	2.548	4.015
Scan type	ω/2θ scan	ω/2θ scan
θ_{max} (°)	70.00	69.81
h,k,l range	$-10 \le h \le 10$ $-16 \le k \le 16$ $-19 \le l \le 19$	$-13 \le h \le 13$ $-15 \le k \le 15$ $-17 \le l \le 17$
Reflections used ($I > 2\sigma(I)$)	6688	4815
$R[F^2 > 2\sigma(F^2)]$, $wR(F^2)$	0.050 2, 0.100 9	0.043 2, 0.111 5
GoF	0.860	0.938

$^3J_{H\text{-}H}$ = 7.7 Hz, H4), 3.49 (m, H3), 3.01 and 2.56 (m, CH_2), 2.18 and 2.03 (m, CH_2), 1.26 (br, BH_3). $^{13}C\{^1H\}$ NMR ($CDCl_3$): 139.7 (d), 138.6 (d), 137.6 (d), 137.6, 137.1, 136.9, 136.8, 136.1, 134.6, 134.5, 134.0 (d), 132.4 and 132.3 (C5 and C6), 123.6 and 122.7 (C4 and C7), 115.0 (m, C1), 107.5 (C2), 68.2 (C3), 22.1 (d, $^1J_{C\text{-}P}$ = 45 Hz, CH_2P), 20.0 (ind-C). $^{31}P\{^1H\}$ NMR ($CDCl_3$): 29.9 (s, PPh_3), 17.1 (br, PPh_2BH_3). Anal. calcd.: C 70.59, H 5.49; found: C 70.22, H 5.55.

Crystal structure determinations[6]

Dark red crystals of **2**·BH_3 and red crystals of **3** were obtained from CH_2Cl_2–hexane solutions kept at –20 °C. The crystal data for **2**·BH_3 and **3** were collected on a Nonius CAD-4 diffractometer with graphite-monochromated Cu Kα radiation at 223(2) K using the CAD-4 software (27). Refinement of the cell parameters was done with the CAD-4 software, while the data reduction used NRC-2 and NRC-2A (28). Both structures were solved by direct methods using SHELXS97 (29) and difmap synthesis (SHELXL96) (30). The refinements were done on F^2 by full-matrix least squares. All non-hydrogen atoms were refined anisotropically, while the hydrogens (isotropic) were constrained to the parent atom using a riding model. Crystal data and experimental details for **2**·BH_3 and **3** are listed in Table 1, and selected bond distances and angles are given in the figure captions.

Acknowledgements

We gratefully acknowledge the Natural Sciences and Engineering Research Council of Canada (NSERC), le fond FCAR of Quebec, and Université de Montréal for financial support. Christophe Valla is thanked for contributing to the preparation of complex **3**.

References

1. D. Zargarian. Coord. Chem. Rev. **233–234**, 157 (2002).
2. (*a*) M.A. Dubois, R. Wang, D. Zargarian, J. Tian, R. Vollmerhaus, Z. Li, and S. Collins. Organometallics, **20**, 663 (2001); (*b*) L.F. Groux, D. Zargarian, L.C. Simon, and J.B.P. Soares. J. Mol. Catal. A, **193**, 51 (2003); (*c*) L.F. Groux and D. Zargarian. Organometallics, **22**, 4759 (2003).
3. R. Wang, F. Bélanger-Gariépy, and D. Zargarian. Organometallics, **18**, 5548 (1999).
4. (*a*) F.-G. Fontaine and D. Zargarian. Organometallics, **21**, 401 (2002); (*b*) F.-G. Fontaine and D. Zargarian. J. Am. Chem. Soc. **126**, 8786 (2004).

[6] Supplementary data for this article are available on the Web site or may be purchased from the Depository of Unpublished Data, Document Delivery, CISTI, National Research Council Canada, Ottawa, ON K1A 0S2, Canada. DUD 3676. For more information on obtaining material refer to http://cisti-icist.nrc-cnrc.gc.ca/irm/unpub_e.shtml. CCDC 269091 and 269092 contain the crystallographic data for this manuscript. These data can be obtained, free of charge, via www.ccdc.cam.ac.uk/conts/retrieving.html (or from the Cambridge Crystallographic Data Centre, 12 Union Road, Cambridge CB2 1EZ, UK; fax +44 1223 336033; or deposit@ccdc.cam.ac.uk).

5. F.-G. Fontaine, R.-V. Nguyen, and D. Zargarian. Can. J. Chem. **81**, 1299 (2003).
6. H. Butenschoen. Chem. Rev. **100**, 1527 (2000).
7. (*a*) A. Döhring, V.R. Jensen, P.W. Jolly, W. Thiel, and J.C. Weber. Organometallics, **20**, 2234 (2001); (*b*) P.W. Jolly, A. Döhring, and J.C. Weber. Patent WO 01002323, 2001.
8. R.J. Whitby. Patent WO 03013724, 2003.
9. (*a*) Y. Kataoka, Y. Nakagawa, A. Shibahara, T. Yamagata, K. Mashima, and K. Tani. Organometallics, **23**, 2095 (2004), and refs. therein; (*b*) Y. Kataoka, Y. Nakagawa, A. Shibahara, Y. Saito, T. Yamagata, and K. Tani. Organometallics, **17**, 4338 (1998); (*c*) D.C. Brookings, S.A. Harrison, R.J. Whitby, B. Crombie, and R.V.H. Jones. Organometallics, **20**, 4574 (2001).
10. C. Charrier and F. Mathey. J. Organomet. Chem. **170**, C41 (1979).
11. Y. Kataoka, Y. Saito, A. Shibahara, and K. Tani. Chem. Lett. 621 (1997).
12. Spirocyclic indenes can be prepared through various routes, e.g., T. Kauffmann, K. Bergus, A. Rensing, and J. Ennen. Chem. Ber. **118**, 3737 (1985), including the base-induced ring-closing reaction of $IndCH_2CH_2Br$.
13. L.F. Groux and D. Zargarian. Acta Crystallogr. Sect. C, **C56**, e366 (2000).
14. (*a*) T.A. Huber, M. Bayrakdarian, S. Dion, I. Dubuc, F. Bélanger-Gariépy, and D. Zargarian. Organometallics, **16**, 5811 (1997); (*b*) F.-G. Fontaine, M.-A. Dubois, and D. Zargarian. Organometallics, **20**, 5156 (2001).
15. The unit cell parameters of a single crystal matched those previously reported for this compound: J.M. Cassidy and K.H. Whitmire. Acta Crystallogr. Sect. C, **C47**, 2094 (1991).
16. T.A. Huber, F. Bélanger-Gariépy, and D. Zargarian. Organometallics, **14**, 4997 (1995).
17. (*a*) L.F. Groux, F. Bélanger-Gariépy, D. Zargarian, and R. Vollmerhaus. Organometallics, **19**, 1507 (2000); (*b*) L.F. Groux and D. Zargarian. Organometallics, **20**, 3811 (2001); (*c*) L.F. Groux and D. Zargarian. Organometallics, **22**, 3124 (2003).
18. For a detailed discussion of slip parameters in various Ind complexes, see: (*a*) R.T. Baker and T.H. Tulip. Organometallics, **5**, 839 (1986); (*b*) S.A. Westcott, A. Kakkar, G. Stringer, N.J. Taylor, and T.B. Marder. J. Organomet. Chem. **394**, 777 (1990).
19. For a comprehensive review on η^1-indenyl complexes, see: M. Stradiotto and M.J. McGlinchey. Coord. Chem. Rev. **219–221**, 311 (2001).
20. For recent reviews on preparation and reactivities of pincer complexes, see: (*a*) M. Albrecht and G. van Koten. Angew. Chem. Int. Ed. **40**, 3750 (2001); (*b*) M.E. van der Boom and D. Milstein. Chem. Rev. **103**, 1759 (2003); (*c*) J.T. Singleton. Tetrahedron, **59**, 1837 (2003).
21. (*a*) S. Niu and M.B. Hall. J. Am. Chem. Soc. **121**, 3992 (1999); (*b*) M. Gupta, C. Hagen, W.C. Kaska, R.E. Cramer, and C.M. Jensen. J. Am. Chem. Soc. **119**, 840 (1999); (*c*) M. Gupta, C. Hagen, R.J. Flesher, W.C. Kaska, and C.M. Jensen. Chem. Commun. 2083 (1996); (*d*) D.W. Lee, W.C. Kaska, and C.M. Jensen. Organometallics, **17**, 5731 (1998); (*e*) M. Gupta, W.C. Kaska, and C.M. Jensen. Chem. Commun. 461 (1997); (*f*) F. Liu and A.S. Goldman. Chem. Commun. 655 (1999); (*g*) F. Liu, E.B. Pack, B. Singh, C.M. Jensen, and A.S. Goldman. J. Am. Chem. Soc. **121**, 4086 (1999); (*h*) C.M. Jensen. Chem. Commun. 2443 (1999).
23. P. Dani, T. Karlen, R.A. Gossage, S. Gladiali, and G. van Koten. Angew. Chem. Int. Ed. **39**, 743 (2000).
23. D. Morales-Morales, C. Grause, K. Kasaoka, R. Redon, R.E. Cramer, and C.M. Jensen. Inorg. Chim. Acta, **958**, 300 (2000).
24. A.L. Seligson and W.C. Trogler. Organometallics, **12**, 744 (1993).
25. (*a*) L.P. Barthel-Rosa, V.J. Catalano, K. Maitra, and J.H. Nelson. Organometallics, **15**, 3924 (1996); (*b*) L.P. Barthel-Rosa, V.J. Catalano, and J.H. Nelson. Chem. Commun. 1629 (1995); (*c*) M.D. Fryzuk, S.S.H. Mao, M.J. Zaworotko, and L.R. MacGillivary. J. Am. Chem. Soc. **115**, 5336 (1993).
26. Y. Kataoka, Y. Iwato, T. Yamagata, and K. Tani. Organometallics, **18**, 5423 (1999).
27. Enraf-Nonius. CAD-4 Software. Version 5.0 [computer program]. Enraf-Nonius, Delft, The Netherlands. 1989.
28. E.J. Gabe, Y. Le Page, J.-P. Charlant, F.L. Lee, and P.S. White. J. Appl. Crystallogr. **22**, 384 (1989).
29. G.M. Sheldrick. SHELXS. Program for the solution of crystal structures [computer program]. University of Goettingen, Germany. 1997.
30. G.M. Sheldrick. SHELXL. Program for the refinement of crystal structures [computer program]. University of Goettingen, Germany. 1996.